System Performance of the Dual-Channel Mu-II Sequential Ranging

W. L. Martin
Communications Systems Research Section

This article discusses the purposes and performance of the Dual-Channel Mu-II Sequential Ranging equipment in both the laboratory and field. Measurements were made to quantify the degradation introduced by the exciter, receiver, Ranging Subsystem, and spacecraft transponder. Additionally, both long- and short-term group delay stability is discussed. Finally, experimental data obtained during the Mariner Venus/Mercury 1973 mission are presented to show the utility of the machine.

I. Introduction

The Dual-Channel Sequential Ranging System (Fig. 1) was designed to support the Mariner Venus/Mercury 1973 (MVM'73) radio science experiments. Experimental objectives included a study of the interplanetary plasma and an investigation of the solar corona.

A radio signal is delayed as it passes through a plasma field. Magnitude of this delay is dependent upon both the field's density and the frequency of the radio wave. Theoretically the differential delay resulting from two radio signals of different frequency passing through a common plasma field is proportional to the ratio of those frequencies squared. Thus, if the frequencies are known, measurement of the differential delay allows the unique solution of field density.

MVM'73 was the first space mission to fly a two-frequency (S- and X-band) ranging transponder. It provided a premier opportunity to measure the total columnar electron density as well as the plasma dynamics. Past missions have been restricted to the latter since they carried a single-frequency (S-band) transponder. While the plasma dynamics are scientifically interesting, the inability to determine total columnar electron density represented a potential source of error preventing the full realization of other experimental objectives.

For example, both the Mariner 1969 and 1971 missions included a relativity experiment wherein the objective was to differentiate between Einstein's theory of general relativity and a modification of that theory proposed by Brans–Dicke.

The experiment consisted of measuring the range over a protracted period in order to establish the spacecraft's orbit with a high degree of confidence. These range measurements continued as the spacecraft passed behind the Sun and the Sun–Earth–probe angle became small, on the order of 1 degree. As the signal's ray path approached the Sun, the intense gravitational field resulted in a warping of the time-space field such as to make the apparent distance appear greater than that predicted by the spacecraft's orbit. This difference is due to the relativistic delay and is the subject of the theories promulgated by Einstein and Brans–Dicke.

Since only 7% separates the delays predicted by the two theories, a high degree of precision is required to differentiate between them. Unfortunately, plasma from the solar corona also introduces a delay in the received signal. While its magnitude is only a small fraction of the relativistic delay, the two are indistinguishable, and the size of the coronal delay is sufficiently large so it cannot be ignored. Thus, models have been formulated which attempt to quantify the coronal delay as a function of Sun–Earth–probe angle. The problem is that these are necessarily steady-state representations which approximate the average expected delay.

On the other hand, the solar corona is actually a highly dynamic body wherein day-to-day variations can reach a substantial fraction of the total coronal delay. Therefore, the modeling technique contains an intrinsic error limiting the accuracy of delay determination and hence the relativity experiment. Clearly, what is needed is an actual, daily, measurement, not only to test the corona model, but also for the correction of range data around superior conjunction. The dual-channel, S–X, ranging equipment provides this capability for the first time. But faith in the measurements made by this device must necessarily depend upon a trust in the ranging machine itself. Therefore, the remainder of this article is devoted to presenting and interpreting test data collected over a period of months with the Dual-Channel Sequential Ranging System.

II. Code Correlation Characteristics

To isolate the components introducing errors, correlation measurements were made in the Telemetry Development Laboratory (TDL) using a variety of system configurations including:

(1) The ranging equipment alone.

(2) The ranging equipment connected to a wide-band 10-MHz modulator.

(3) The ranging equipment connected to a Block III Receiver/Exciter Subsystem using a wide-band zero-delay device.

(4) The ranging equipment connected to a Block III Receiver/Exciter Subsystem using an MVM'73 prototype transponder.

Figure 2 pictorially summarizes the four test configurations. Correlation curves are generated by connecting the equipment in one of the four modes. After acquiring the range in a normal manner, the local reference (receiver) coder is shifted by its smallest increment (7.5 or 15 nanoseconds depending upon the reference frequency), and a new phase measurement is made. This process of shift and measure is continued through one complete code cycle. Both the 0- and 90-degree accumulators are integrated over the period of each phase measurement, and this number, representing the degree of correlation, is recorded at the conclusion of the measurement.

When plotted, the two channels represent the familiar code correlation curves (see Fig. 3). Of course, Fig. 3 represents a theoretical, and hence idealized, correlation function. In actuality, bandpass limitations and non-uniform phase shifts between the fundamental code frequency and its harmonics cause a distortion of the correlation relationship. These nonlinearities can result from imperfections in the ranging equipment itself, or from code waveform distortion occurring within the associated Deep Space Station (DSS) Receiver/Exciter Subsystem or within the spacecraft's transponder. Thus, the purpose of these tests was to investigate the contribution of each aforenamed subsystem to total system error. During the first test, the Ranging Subsystem's transmitter code output was connected, through an attenuator, to its receiver 1 input. Because of the automatic gain control (AGC) amplifier's wide-band characteristics, the range code is passed directly through to the analog-to-digital converter and thence to the correlator. To foreclose a significant droop in the range code due to the amplifier's low-frequency cutoff, a 2-MHz code was selected for this test.

Under normal operating conditions the equipment receives a 10-MHz carrier, phase modulated with the ranging code. Where as here the code is present without the 10 MHz, correlation against a model containing a 10-MHz reference will result in the integral of samples over the interval being zero. Thus, the internal reference must be disabled. Fortuitously, this can easily be accomplished via the 10-MHz disable switch conveniently located on the machine's front panel.

Figure 4 summarizes the results of the "base band" test. Since a 2-MHz code, rather than the usual 500-kHz code, was used for this test, only 32 steps were required to shift its phase through one complete cycle. This resulted in a rather large spacing between points, as will be observed in the quadrature channel where the individual steps are plotted, and accounts for the roughness of the solid curve.

Note that the spacing of the peak points is different from all others. This is due to the local (receiver) code never being perfectly in phase with the transmitter code because the 15-nanosecond shift available with a 66-MHz reference is too coarse. Thus, the correlator output at this point is less than it would have been had the 2 codes been in phase. This causes an apparent distortion in the correlation curve which is not actually present in the machine and is one of the reasons why a 132-MHz reference was selected in preference to the 44-MHz alternative available from the Block IV exciter. In the presence of noise this apparent quantization does not reduce the accuracy of the range measurement.

The intrinsic accuracy of the machine is determined by the linearity of the correlation curve, for it is this relationship between reference and quadrature channels that translates into a phase measurement. Linearity in turn is affected by, among other things, code waveform both within and without the machine. It is useless to generate a perfect transmitter code and an ideal modulator, exciter, and spacecraft transponder if the local code used for correlation purposes is defective, for the result is but the product of the two waveforms and the poorer will prevail. Thus, when one asks a 1-nanosecond accuracy in range, he is requiring a phase measurement to be better than 0.05%, placing stringent requirements on code waveforms.

As discussed earlier, precision and stability were primary objectives. They were achieved by providing wide bandwidths and careful control over all code waveforms. High-speed logic was used to ensure that transition times were short and symmetry was good.

Comparing the phase calculated using the measured correlation curve (Fig. 4) with that obtained with a perfect square wave (and hence an ideal correlation function), yields the error curve of Fig. 5. Note the peaks occurring at $\pi/2$ intervals due to the distortion in the correlation function at its maximum and minimum values. As discussed supra, this distortion is a product of the quantization and delay experienced in this particular test and would be expected to disappear under normal operating conditions. Thus, the slight difference in amplitude of the error function due to slightly greater distortion in the reference channel would also probably disappear.

The important information presented by Fig. 5 can be summarized as follows: First, the error function is substantially periodic at $\pi/2$ intervals. Second, the error at the actual tracking point $(\pi/4 + n\pi/2)$ is virtually nonexistent. Third, the average value over 2π is approximately zero, showing the machine contains no biases. Fourth, the maximum error experienced was on the order of 2 nanoseconds and this was probably due to quantization.

In order to ascertain the degradation in performance resulting from the interconnection with other equipment, similar tests were run using a more normal operating mode. Figure 6 shows the test results using the 10-MHz wide-band modulator (see Fig. 2). This is similar to the previous test in that only the ranging equipment is under test; however, now the input is receiving a 10-MHz phase-modulated carrier as it does when connected with a DSS receiver. Additionally, the typical 500-kHz range code is employed rather than the 2-MHz code.

Observe the high degree of linearity in the sides of the correlation function. The slight rounding at the peaks is due to bandpass restrictions in the modulator; however, this distortion is small compared with that which appears using other configurations.

The error function, Fig. 7, is plotted for one-half of the period (0 to π). Its maximum amplitude is approximately the same as that measured during the baseband test and occurs at the peaks of the correlation function. At other locations the error is substantially zero. Figure 7 also includes an apparent negative bias that results from the method by which code phase is established. In fact, it is part of the system delay that has not been removed and therefore should be ignored.

Continuing with the system tests, Fig. 8 is a plot of the correlation function when the system is connected to a standard DSS Block III Receiver/Exciter Subsystem through a zero-delay device (refer to configuration diagram Fig. 2). A zero-delay device comprises a wide-band crystal mixer which converts a part of the transmitted energy to the receive frequency and is so named because its through-put time is exceedingly small.

Careful inspection of Fig. 8 reveals some nonlinearity in the correlation function. This is likely due to a non-uniform shift in the phase of the higher-order range code harmonics with respect to the fundamental frequency. Note, also, the somewhat greater rounding at the peaks of

the correlation curves. This is consistent with the non-uniform phase-shift theory in that the rounding is indicative of poor high-frequency response in the system. As the response begins to roll off, it becomes uneven with the result that the phase-frequency characteristic is nonlinear. This in turn results in a disproportionate phase shift in the high-order harmonics and the nonlinear correlation curve.

The effect is clearly evident in the error curve of Fig. 9. Here the amplitude has increased from approximately 2 nanoseconds to more than 7 nanoseconds. Note, also, that the area under the error function is substantially greater than that indicated in Figs. 5 and 7. This results not only from the increased amplitude, but, also, from an increase in the error value at all code phases. The latter results from the nonlinearity in correlation function caused by non-uniform harmonic phase shift.

The final system test results appear in Fig. 10. For this measurement a Block III exciter was connected to a Block III receiver via the MVM'73 prototype transponder (see Fig. 2). This, then, represents a hardware complement similar to that which would be found in the field during an actual mission track. The tests were run at relatively strong ranging signal levels in order to properly identify the system's characteristics. However, the total uplink power was kept at −120 dBm in order to ensure a noise-limited condition at the spacecraft transponder's limiter and, hence, linear performance (i.e., no material reconstruction of the range code).

Here the degradation is readily apparent by comparing Fig. 10 with any of the preceding correlation curves. Not only has the linearity suffered badly, but, also, the peak-rounding is so great that the curve is becoming nonlinear at the equal power points for the reference and quadrature channels. Moreover, careful inspection reveals that this rounding is asymmetrical with respect to the true peak. Again, this follows from the restricted bandwidth; however, in this case the spacecraft is the limiting element.

The degradation is clearly evident in the error function (Fig. 11). Amplitude is some 8 times greater than that measured in the baseband test. Moreover, the magnitude remains fairly high for all code phases, indicating substantial high-order harmonic phase shift. Further indication of this shift appears from the asymmetrical character of the error curve, that is, the sharp increase followed by the relatively slow decline. The message here is that the correlation function is not symmetrical with respect to its peak, with the result that the optimal tracking point has been shifted from the normal, $\pi/4$, point.

Examination of Fig. 10 reveals that the once triangular correlation curve now approximates a sine wave. Some possibilities for improvement in system performance suggest themselves. It is obvious from the foregoing discussion that the greatest degradation occurs in the transponder. This means that the transponder's characteristics of bandwidth and harmonic phase shift are the dominant factors in shaping the correlation curve and, hence, the overall system performance. From here it follows that small variations in ground equipment bandwidth will not affect system delay since the transponder's relatively narrow bandwidth will have removed most code harmonics. Thus, the spacecraft's characteristics dominate, and, if a method could be found to quantify the distortion introduced by the transponder, the overall ranging accuracy could be improved.

One method is to measure the correlation characteristics of each transponder as was done here with the MVM radio (Fig. 10). These measurements can be incorporated as corrections to the linear phase estimator algorithm employed in the ranging system. Using this technique the ranging equipment could be exactly matched to each spacecraft.

A second alternative is to filter the higher-order harmonics between the DSS receiver and the ranging equipment. In this case the phase shift introduced in the harmonics by the transponder is unimportant since only the fundamental remains after the filtering. Preliminary tests show that, when used in conjunction with an arc tangent phase estimator algorithm, the filtering method reduces errors to about the level of the ranging equipment alone.

Both alternatives are under active investigation. Unless dramatic improvements in transponder design are forthcoming, one of them will probably be necessary to meet the accuracy requirements of future missions.

III. System Stability

Another aspect of accuracy is stability. By this is meant the system's ability to produce the same result over a period of time where conditions remain relatively unchanged. Stability can be further subdivided into short-term and long-term components.

Short-term stability may be defined as the capacity to remain invariant over periods from 8 to 12 hours, such as

would be experienced during a single pass. This characteristic is important because the equipment is only calibrated prior to, and occasionally after, each track. Changes occurring during the pass are indistinguishable from the parameter being measured, either range, or the change in range due to particle dynamics (DRVID). These variations impose an upper bound on the system's accuracy and every effort should be made to minimize them.

Long-term stability refers to the system's ability to produce consistent results over a period of months. This is, of course, inexorably related to short-term stability in many respects, for most of the factors influencing one will also affect the other. Frequently, a situation will arise which forecloses a ranging calibration either prior to or following a pass. The reasons can vary from overcommitment of station tracking time to equipment malfunctions that require repair during the normal calibration periods. In a situation such as this, it is desirable to use the calibration of the previous day or, perhaps, of the previous week if tracks are infrequent. This is only possible if the delay will not have changed during the period and therefore long-term stability becomes very important.

As noted in an earlier section, considerable care was taken to ensure high stability in the Ranging Subsystem. To evaluate the success of this effort, the range code was connected, via the wide-band 10-MHz modulator, to the ranging unit's input (see Fig. 2). This utilized the minimum amount of external equipment necessary to make a meaningful stability measurement.

A normal range acquisition was made and the machine was allowed to continually remeasure the range at 10-minute intervals for more than 16 hours. The results are plotted in Fig. 12. During the entire period the peak-to-peak variation was less than 60 picoseconds (60×10^{-12} seconds). Moreover, the average variation during the same period was on the order of 30 picoseconds. This corresponds to a change in one-way range of less than 1/4 inch (approximately 5 millimeters) over the 17-hour period!

While the relative contributions of the modulator and Ranging Subsystem are inseparable, the size of the change probably makes further consideration of this matter unnecessary. Unless one is willing to postulate larger drifts in opposite directions for each piece of equipment, which almost perfectly compensate one another, and which situation is highly unlikely, then the only conclusion left is that neither equipment changes significantly.

Long-term stability of the *entire ground system* was evaluated by plotting ranging calibration data obtained at DSS 14 over a period of several months. The particular configuration consisted of the Ranging Subsystem herein described, a standard Block III exciter and the new Block IV receiver. The zero-delay device at DSS 14 had been improved so as to eliminate the air path and therefore a problem with RF reflections which had been found near the face of the dish.

The calibrations, made at S-band, are plotted in Fig. 13 for a period from February through the middle of June 1974. Because of different path lengths, only data obtained with the 100-kW transmitter were plotted.

Note the remarkable consistency throughout the entire period. The average delay was found to be 3.470 microseconds and the standard deviation was less than 4 nanoseconds (approximately 1/2 meter in one-way range). One can discern evidence of cyclic behavior whose period is approximately 25 days. After the system had stabilized following day 70, the day-to-day variation is extremely small compared with the cyclic characteristic. Some effort should be expended to identify the source of this change, whereafter the total variation (peak-to-peak) could probably be reduced to less than 5 nanoseconds. If this were done, daily calibration may be found unnecessary.

As a further check on long-term stability, differential group delay was plotted for a somewhat longer period using both the 100- and 20-kW transmitters. The results appear in Fig. 14. Here the data can be separated into three distinct groups. During the early part of the year, just prior to Mercury encounter, there was considerable activity at DSS 14 in readying the new Block IV receiver for the critical period. The effect of this activity is evident as an increased instability in differential delay prior to day 70.

On or about day 75, cables traversing the elevation bearing were replaced, resulting in a substantial change in differential delay. Thereafter, the day-to-day variation became smaller and the cyclic behavior more evident. From day 80 through day 135 the average delay diminished by only 1 nanosecond, although the periodic signature resulted in a standard deviation of about 4.5 nanoseconds.

The station was inactivated for a period of time following day 135. During this period certain unidentified changes took place, causing the differential delay to decrease by 6.7 nanoseconds. This reconfiguration also appears to have had a stabilizing effect in that the average

delay remained unchanged during the following 1-1/2 months. Moreover, the cyclic variation appears to be increased in frequency and reduced in amplitude. Thus, careful scrutiny of the alterations made during this period may provide a clue as to its cause.

The conclusion reached from this compendium of information is that the entire ground system exhibits fairly stable behavior over substantial periods of time, particularly if left undisturbed. Further work should be undertaken to identify the source of the cyclic behavior.

IV. Experimental Results

In the final analysis, the test of any system is in the utility of information which it produces. As noted in the introduction to this section, one limitation on the accuracy of relativity experiments has been the absence of a dynamic corona model. Obviously, the best model is obtained from actual measurements made through the time near superior conjunction.

The two-frequency capability of this system provided a unique opportunity to measure not only the dynamics but also absolute coronal delay. The effect of the solar corona upon group delay will be found in Fig. 15 and is presented through the courtesy of T. Howard of Stanford University, team leader of Mariner 10 Radio Science Experiments.

No attempt will be made to interpret these data, which are far beyond the purpose or scope of this presentation. Suffice it to say that the graph amply demonstrates the system's ability to resolve not only the magnitude of delay but, also, its day-to-day variation. Theoretical computations have confirmed the correctness of the data contained in the figure.

One final measurement deserves mention. On day 171, approximately 2 weeks after superior conjunction, the ranging equipment was configured to provide rapid, multiple acquisitions. Only three range code components were employed, which were sufficient to resolve the differential delay resulting from the solar corona. Some 25 points were obtained over a 4-hour period, approximately one point every 10 minutes. The purpose here was to demonstrate the machine's ability to resolve high-frequency fluctuations in coronal density, which caused changes in differential group delay. The data are plotted in Fig. 16.

The predicted signal level available on day 171 was such that the expected variation in delay due to noise was small compared with the changes actually observed. Again, interpretation of these data is not within the purpose of this work, and the data are included simply to show the capabilities of the equipment.

V. Conclusions

All this leaves a question as to what can and should be done to improve the entire system's accuracy. The foregoing evidence suggests several conclusions.

First, the ranging equipment, standing by itself, appears quite adequate. The tests have shown that improvements in this subsystem would not materially affect the overall system performance.

Second, accuracy and stability with the Block III Receiver/Exciter Subsystem are fairly good. While bandwidth limitations are clearly present and some nonlinearity exists due to non-uniform harmonic phase shift, these distortions do not appear to have a substantial effect on stability. Work should be undertaken to eliminate the non-uniform phase shifts that probably occur within the exciter. Because it was unavailable for many of these tests, no conclusions are reached with respect to performance with the Block IV equipment.

Third, the dominant source of error is within the spacecraft's transponder. From this it follows that the maximum yield in terms of performance improvement for manpower invested would be obtained by concentrating on this unit.

If one accepts these conclusions as true, then the only reasonable course is in terms of spacecraft transponder development. To attempt alternate "fixes" with respect to the ground equipment is to treat symptoms and not causes, and it will prove both expensive and relatively unproductive in the long term. The underlying problem is one of bandwidth. It is too narrow. A limited bandwidth may have had merit in the days of the 26-m (85-ft) antennas, 10-kilowatt ground transmitters, and pseudonoise ranging systems. Today there are 64-m (210-ft) antennas, 100-kilowatt transmitters, and sequential ranging equipment, and the relevant considerations have changed accordingly. Now the question is no longer whether we can measure range at all, but, rather, how accurately can we measure it. Whereas a 20-meter accuracy was sufficient but a few years ago, now uncertainties greater than 5 meters can invalidate whole experiments. Tomorrow the requirements will press to a few centimeters.

Viewed from this perspective the answer seems clear: widen the bandwidth. Increasing the present 1.5-MHz transponder bandwidth to 12 MHz would result in less than a 10-dB loss in signal-to-noise ratio. To produce the same uncertainty in phase, the already short integration time would have to be increased by a factor of 8, provided that the code frequency remained constant. However, if channel bandwidth limitations imposed by the Federal Communications Commission permitted, the code frequency could, and should, be increased. Remembering the equation for phase uncertainty (Ref. 1)

$$\sigma = 2T[N_0/(2st)]^{1/2}$$

where T is the code bit period.

It is obvious that increasing the code frequency to 2 MHz will result in the same phase noise without changing integration time! But, the higher code frequency will have resulted in improved accuracy for the reason that time, and hence range, has been quantized into smaller units. Thus, the answer is not one of patching an existing and outmoded system, but rather in re-evaluation and change of that system in light of today's experimental requirements.

Acknowledgments

We wish to acknowledge the invaluable assistance of L. Brunn and the personnel at the Telecommunications Development Laboratory for their contributions in obtaining and interpreting this information. Also, special thanks to T. Komarek for providing and allowing publication of the correlation and error plots used in the ranging channel distortion study, and to the personnel at DSS 14 for their aid in operating this system and collecting the group delay stability data.

Reference

1. Goldstein, R. M., "Ranging With Sequential Components," in *The Deep Space Network*, Space Programs Summary 37-52, Vol. II, pp. 46–49, Jet Propulsion Laboratory, Pasadena, Calif., July 31, 1968.

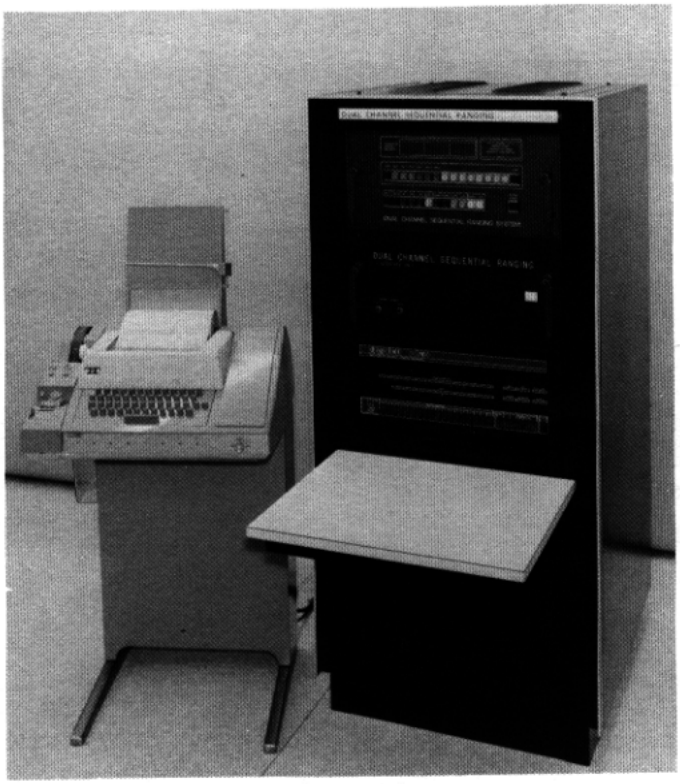

Fig. 1. Dual-Channel Sequential Ranging System

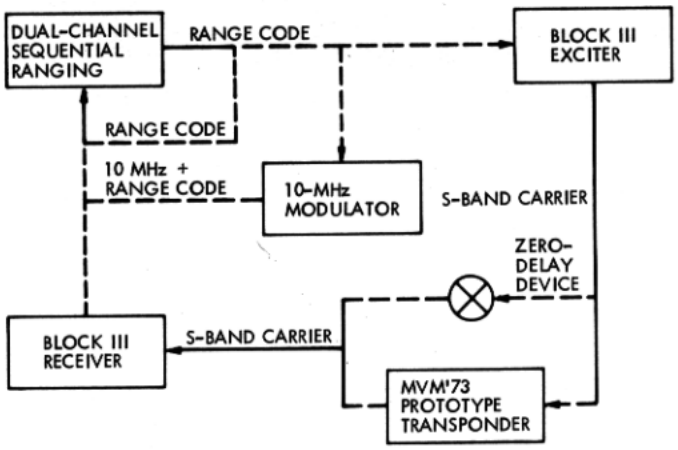

Fig. 2. Ranging test configuration

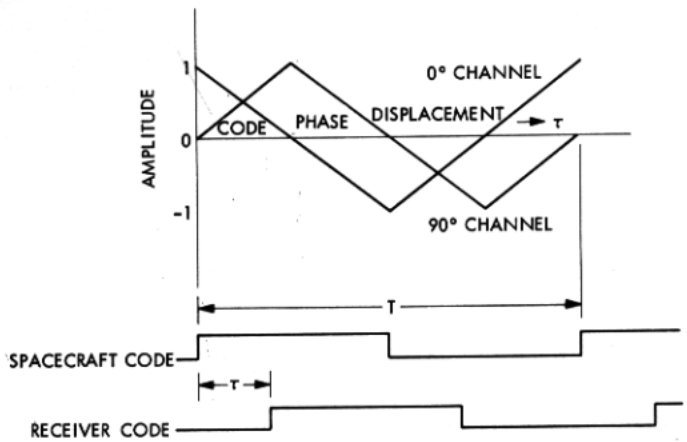

Fig. 3. Theoretical code correlation characteristics

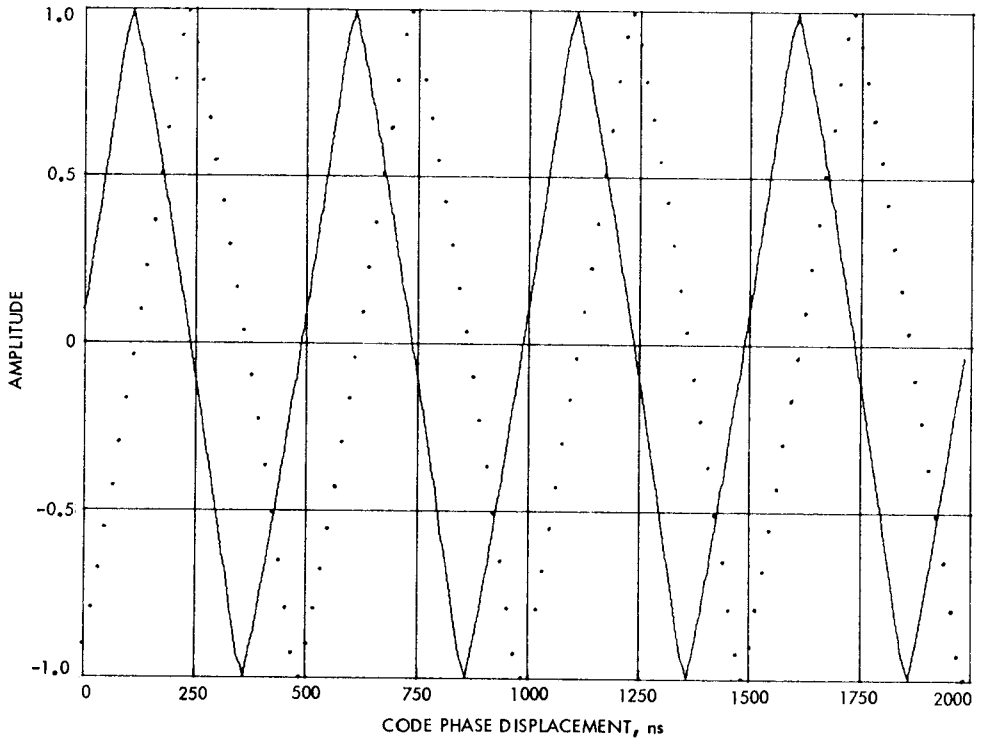

Fig. 4. 2-MHz code correlation characteristics

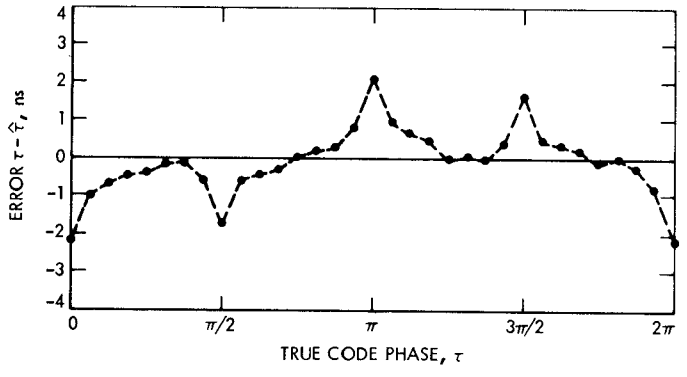

Fig. 5. Error in tau estimate for 2-MHz code baseband test

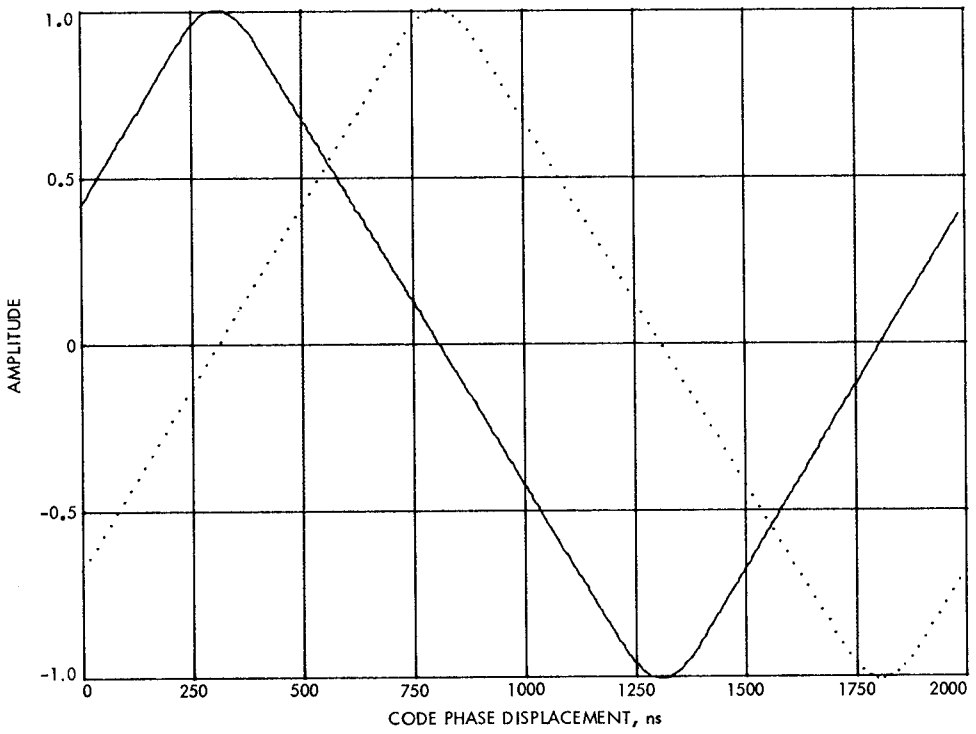

Fig. 6. 500-kHz code correlation characteristics using wide-band modulator

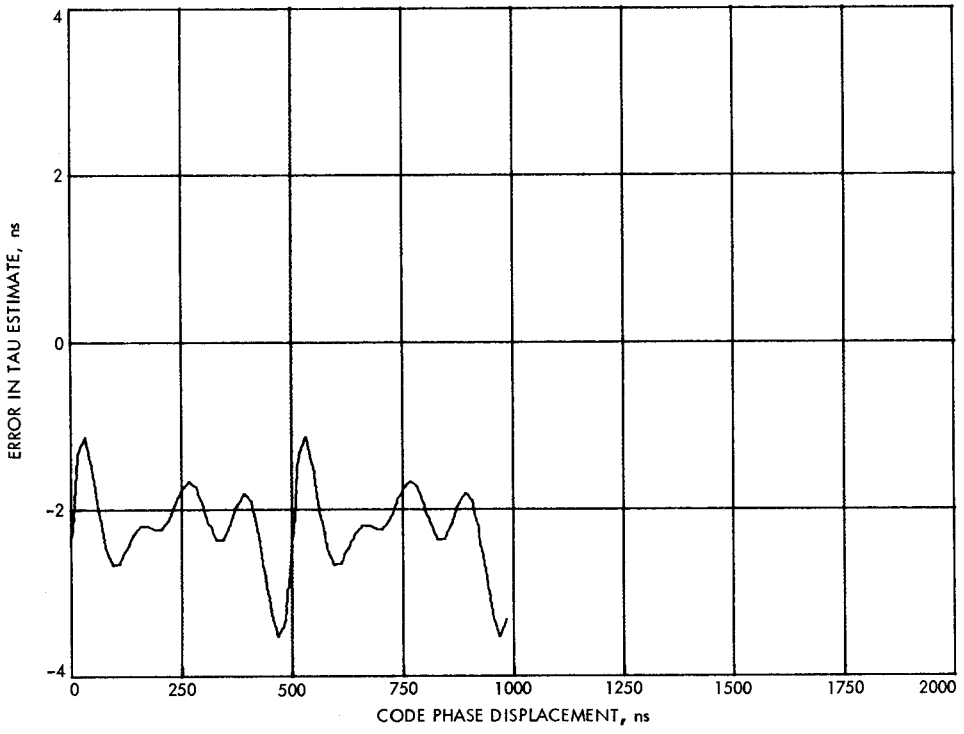

Fig. 7. Error in tau estimate, 500-kHz code using wide-band modulator

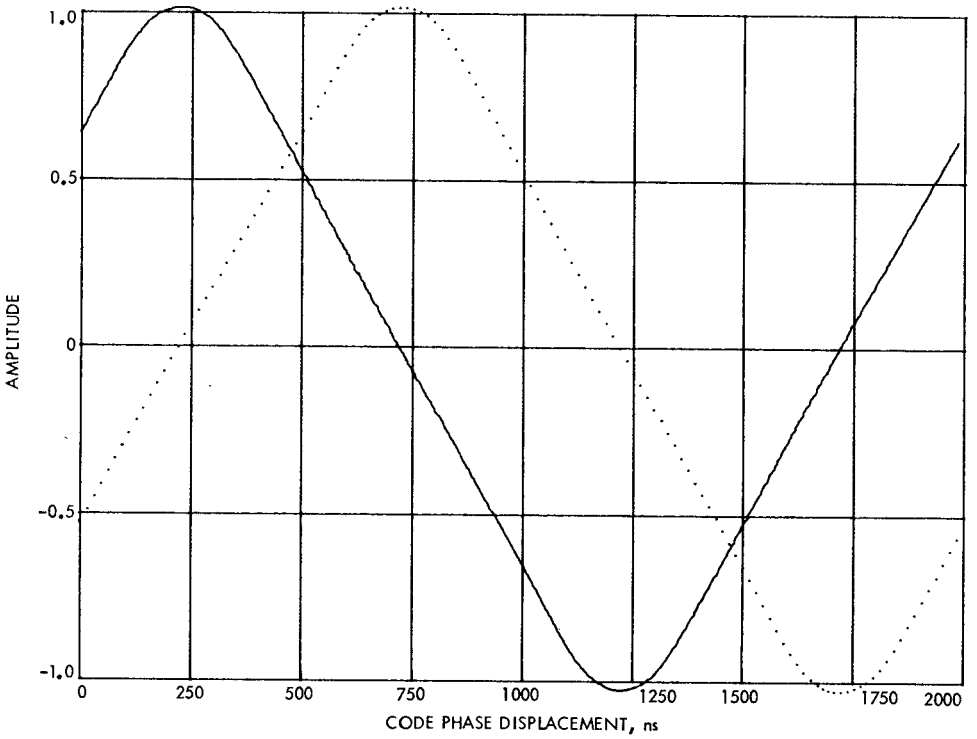

Fig. 8. 500-kHz code correlation characteristics using Block III receiver–exciter/zero-delay configuration

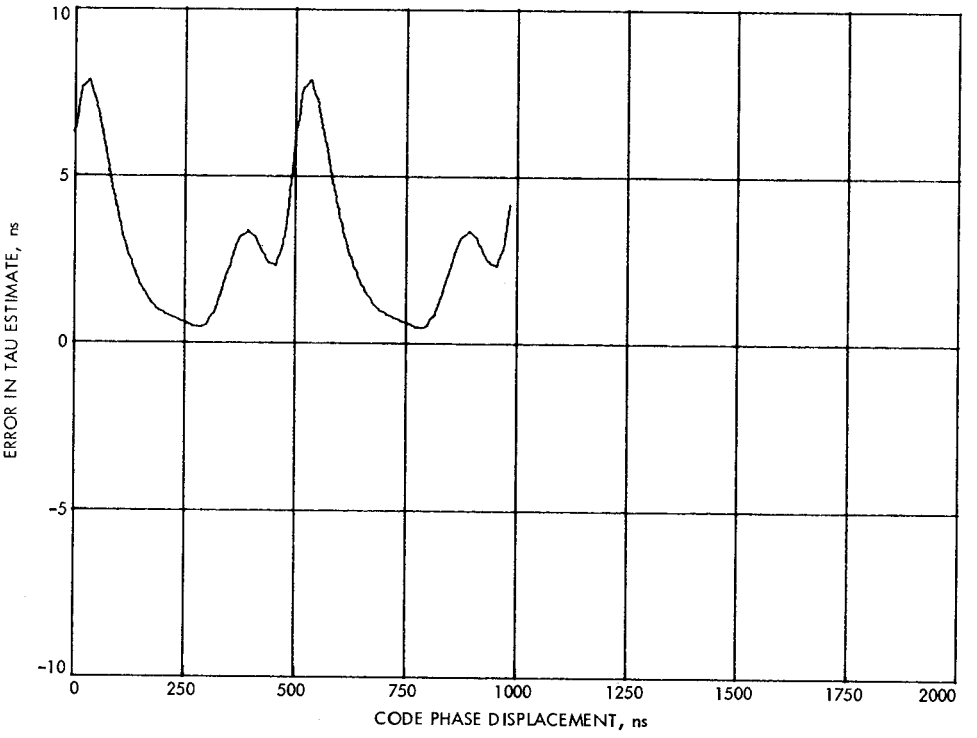

Fig. 9. Error in tau estimate with 500-kHz code using Block III receiver–exciter/zero-delay configuration

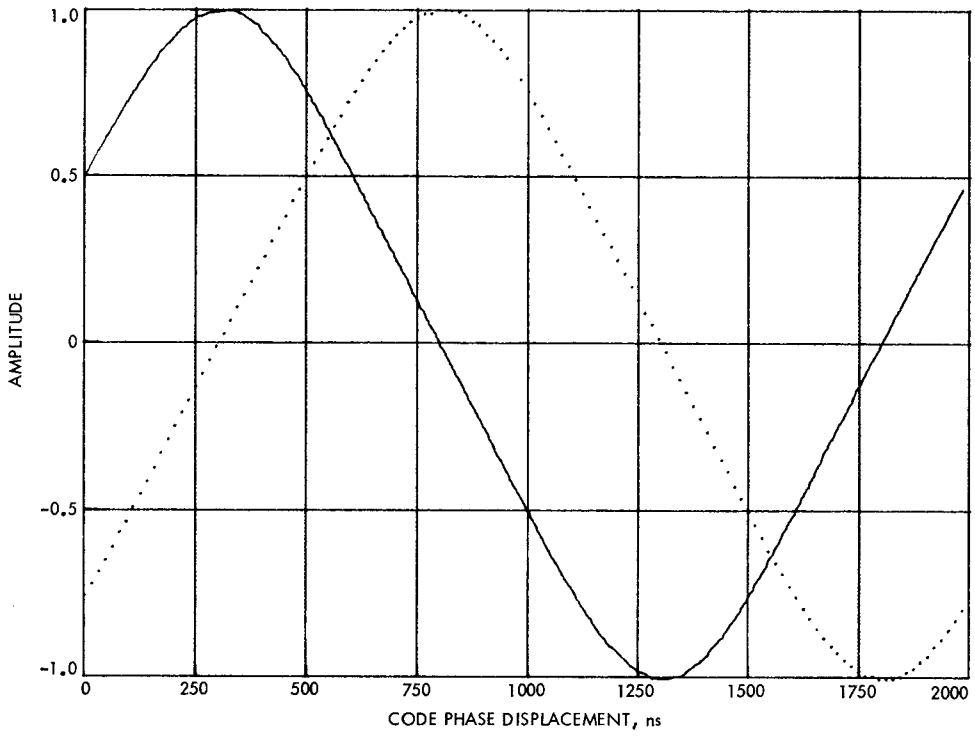

Fig. 10. 500-kHz code correlation characteristics using Block III receiver–exciter/MVM transponder configuration

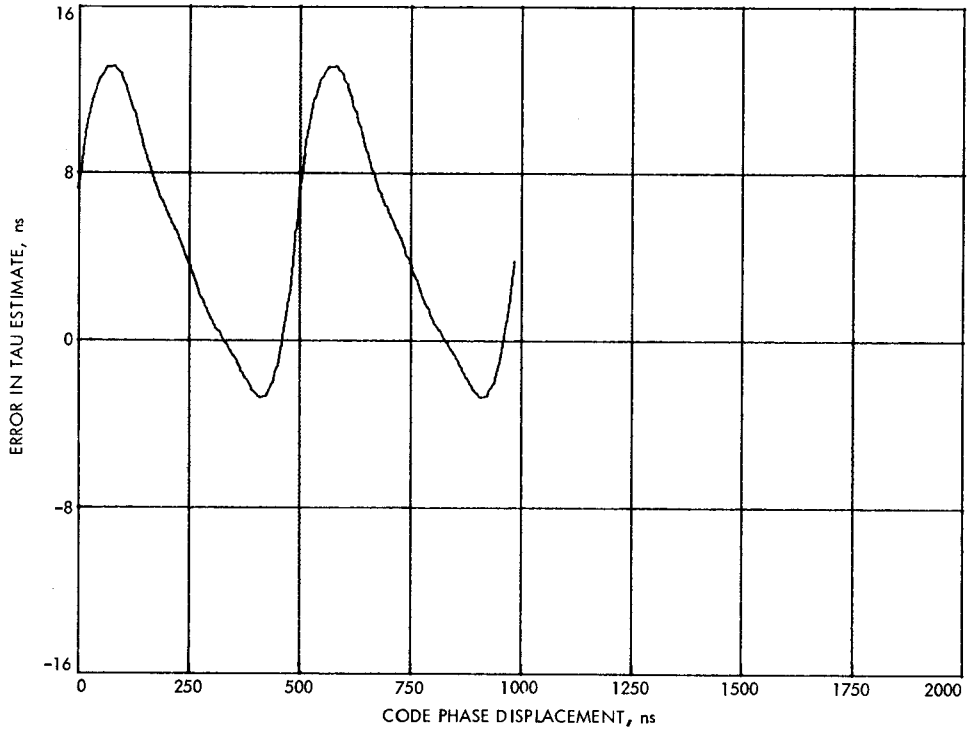

Fig. 11. Error in tau estimate with 500-kHz code using Block III receiver–exciter/MVM transponder configuration

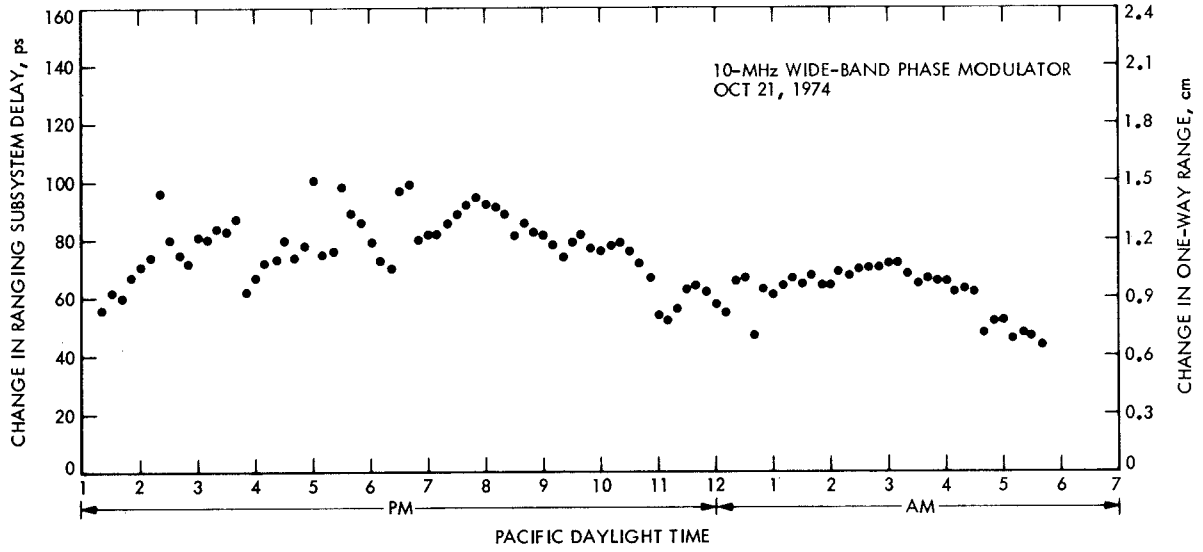

Fig. 12. Results of Ranging Subsystem stability test

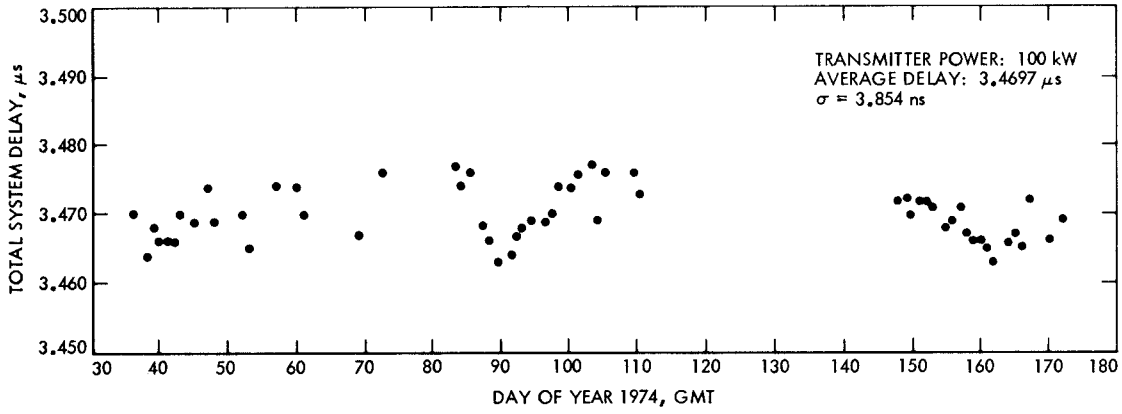

Fig. 13. Mu-II S-band ranging zero-delay calibrations at DSS 14 using Block IV receiver and Block III exciter

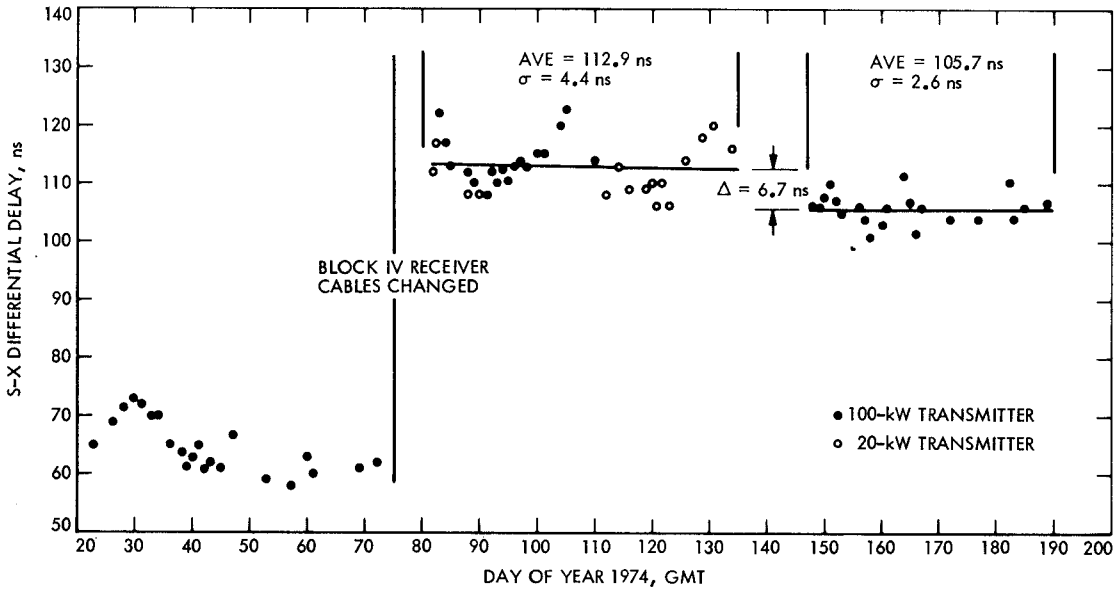

Fig. 14. S−X differential zero-delay calibrations at DSS 14 using Block IV receiver and Block III exciter

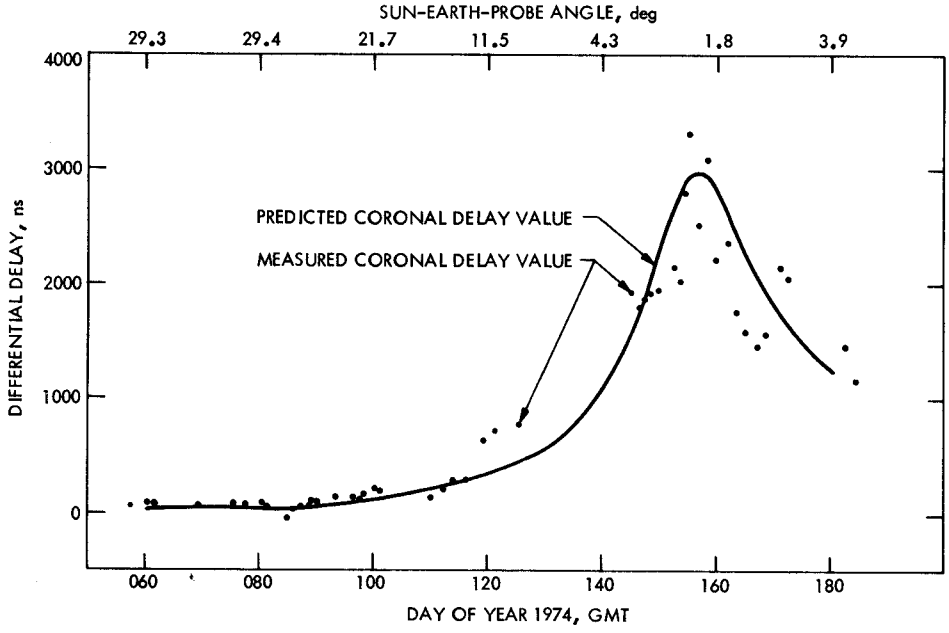

Fig. 15. Mariner 10 S−X differential range at DSS 14

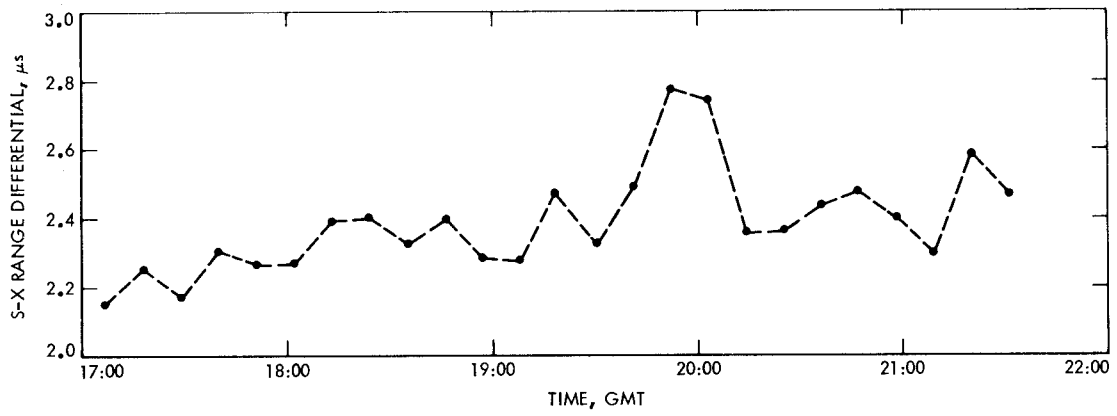

Fig. 16. Coronal dynamics measured by differential range on day 171, 1974